Joint Assignment of Power, Routing, and Spectrum in Static Flexible-Grid Networks

Joint Assignment of Power, Routing, and Spectrum in Static Flexible-Grid Networks

Li Yan, *Student Member, IEEE,* Erik Agrell, *Senior Member, IEEE,*
Madushanka Nishan Dharmaweera, *Member, IEEE*, Henk Wymeersch, *Member, IEEE*

***Abstract*—This paper proposes a novel network planning strategy to jointly allocate physical layer resources together with the routing and spectrum assignment in transparent nonlinear flexible-grid optical networks with static traffic demands. The physical layer resources, such as power spectral density, modulation format, and carrier frequency, are optimized for each connection. By linearizing the Gaussian noise model, both an optimal formulation and a low complexity decomposition heuristic are proposed. Our methods minimize the spectrum usage of networks, while satisfying requirements on the throughput and quality of transmission. Compared with existing schemes that allocate a uniform power spectral density to all connections, our proposed methods relax this constraint and, thus, utilize network resources more efficiently. Numerical results show that by optimizing the power spectral density per connection, the spectrum usage can be reduced by around 20% over uniform power spectral density schemes.**

***Index Terms*—Resource allocation, nonlinear channel, power optimization, flexible-grid optical network.**

I. Introduction

EXPANDING data volumes and an increasing diversity of traffic requests have pushed the development of optical backbone networks towards flexible grids due to their efficient utilization of network resources. In flexible-grid optical networks, the spectrum of each fiber is divided into subcarriers with smaller bandwidth [1]. To further increase resource utilization, a variety of modulation formats can be adopted in these networks. Moreover, by considering the network condition, the physical layer impairments (PLIs), and the requirements of communication demands, resources can be allocated more adaptively to traffic connections.

Since the allocated resources in flexible-grid networks are more heterogeneous than those in traditional fixed-grid wavelength-division multiplexing (WDM) networks [1], connections assigned with various routes, modulations, bandwidths, and power spectral densities (PSDs) can coexist in the same fiber link, resulting in more complicated and significant nonlinear interference (NLI) among connections. Traditionally, to ensure the satisfactory quality of transmission (QoT), different modulation formats are assigned predefined maximum transmission reaches [2]–[4], and fixed guardbands are provisioned between connections [5], [6]. As a result, network resources are used inefficiently.

Recently, adaptive resource allocation algorithms considering various practical issues in network operations have been proposed [7], [8]. However, these algorithms do not consider the transmission power explicitly and, thus, leave one degree of freedom in the optimization unexploited. Algorithms dealing with PSD allocation have been developed [9]–[12] taking into account the interaction between flexible resources and NLIs. However, these algorithms assume a uniform PSD for all the connections and the PSD is optimized separately from other resources due to computational difficulties. Power optimizations in optical networks with precalculated routing and spectrum assignment (RSA) schemes have been proposed [13]–[15], which yield only suboptimal resource allocation due to the separate optimization of power and other resources. Joint individual power and RSA optimization in nonlinear WDM networks [16]–[18] demonstrating improved network throughput have also been studied. However, these algorithms are designed specifically for WDM networks and cannot be applied to flexible-grid networks where connection bandwidths are not uniform.

In this paper, we jointly optimize the PSD of each individual connection with other resources in meshed flexible-grid optical networks. This joint optimization is presented both in the form of a mixed integer linear programming (MILP) formulation and a decomposition heuristic through linear approximations of the nonlinear channel model. The numerical results demonstrate that our proposed algorithms can reduce the bandwidth usage significantly compared to uniform PSD schemes.

The remainder of this paper is organized as follows. In Section II, the resource allocation problem is introduced. The nonlinear PLI model and its linearization are explained in Section III. We present the proposed MILP and heuristic in Section IV. Section V discusses numerical results of the proposed methods for both small and large networks. Concluding remarks are found in Section VI.

II. Problem Statement

In this paper, we consider a transparent optical network represented by a graph with sets of nodes V and links E. Each link has two fibers that carry traffic in opposite directions. Without loss of generality, we assume that the spectrum on each fiber is sliced into subcarriers with a bandwidth of 12.5 GHz [19], and transponders at each node are based

Manuscript received XXX. xx, 2016; revised XXX. xx, 2016; accepted XXX. xx, 2016. Date of publication XXX. xx, 2016; date of current version XXX. xx, 2016.

Part of this paper was presented at the European Conference on Optical Communication (ECOC), Valencia, Sept. 2015.

Research supported by the Swedish Research Council under Grant No. 2012-5280. The authors are with Chalmers University of Technology, SE-41296 Gothenburg, Sweden ({lyaa,agrell,nishan,henkw}@chalmers.se).

Table I
THE AVAILABLE MODULATION FORMATS, THEIR SPECTRAL EFFICIENCIES $c \in M$, AND LINEAR SCALE SNR THRESHOLDS $\text{SNR}^{\text{TH}}(c)$ TO ACHIEVE A PRE-FEC BER OF 4×10^{-3}.

Modulation Format	c (bit/s/Hz)	$\text{SNR}^{\text{th}}(c)$
Polarization-multiplexing (PM) binary phase shift keying (BPSK)	2	3.52
PM-quadrature phase shift keying (QPSK)	4	7.03
PM-8 quadrature amplitude modulation (QAM)	6	17.59
PM-16QAM	8	32.60

on Nyquist WDM technology [20]. However, our proposed resource allocation algorithms are applicable to transmission schemes that are covered with good accuracy by the Gaussian noise (GN) model [21]–[23] and Nyquist WDM is assumed only for convenience. A static traffic scenario is considered, where D is the set of connections. A connection $i \in D$ is characterized by its source s, destination d, and data rate R_i (in Gbps) including FEC overhead for $s \neq d$ and $s, d \in V$. Depending on the traffic load, there can be one or multiple connections for the same source–destination pair. The available modulation formats are listed in the first column of Table I. The set of their spectral efficiencies are denoted as $M = \{2, 4, 6, 8\}$ and is given in the second column of Table I. Higher-order modulation formats are helpful in improving the network utilization, especially in small-diameter networks. However, modulation formats higher than 16-QAM are not considered in this paper to simplify the numerical simulations. Since the spectral efficiencies $c \in M$ are different, we can also use c to denote the corresponding modulation format for convenience. For each available modulation format, its required minimum SNR threshold $\text{SNR}^{\text{th}}(c)$ for $c \in M$ under a certain preforward error correction (FEC) bit-error rate (BER) requirement (4×10^{-3} in this paper) [16] is given in the third column of Table I.

Under the assumption of Nyquist spectral shaping [24], connection $i \in D$ with data rate R_i has bandwidth $\Delta f_i = R_i / c_i$, where $c_i \in M$ is the spectral efficiency of the modulation format used by i. Other resources allocated to connection i include the PSD G_i, the carrier frequency f_i, and a route consisting of a sequence of links connecting the source s_i and destination d_i. The number of spans propagated by connection i along the designated route is denoted by N_i^{span}, and N_{ij}^{span} denotes the number of spans shared by the routes of connections i and j. We assume that the dispersion effects are compensated by the digital signal processing and will not be considered in the PLIs. Therefore, the connection QoTs can be estimated based on the allocated resources by using the GN model [14], [23].

Based on the above-mentioned description, our resource allocation algorithms take as input parameters: the network topology (V, E), set of available spectral efficiencies M, and traffic demands R_i for all $i \in D$. The output of the algorithms consists of carrier frequency f_i, connection bandwidth Δf_i, and PSD G_i for all $i \in D$ and the routes, spectral orderings, and modulation formats, which are given by binary variables p_{il}, u_{ij}, and m_{ic}, respectively, to be defined in Table II.

III. NONLINEAR PHYSICAL LAYER MODEL AND LINEARIZATION

The GN model is an analytical model to calculate NLIs in dispersion-uncompensated fiber links [21]–[23]. In the GN model, NLIs between connections propagating in the same fiber link caused by the Kerr effect are modeled as additive Gaussian noises, which combine incoherently with the additive spontaneous emission (ASE) noise introduced by fiber amplifiers [22], [23], [25]. By combining various PLIs, we can obtain the SNR of connection i, for all $i \in D$, as

$$\frac{G_i}{G_i^{\text{ASE}} + G_i^{\text{SCI}} + G_i^{\text{XCI}}} \geq \text{SNR}^{\text{th}}(c_i), \tag{1}$$

where G_i, G_i^{ASE}, G_i^{SCI}, and G_i^{XCI} are the PSD, ASE noise, self-channel interference (SCI), and cross-channel interference (XCI) of connection i, respectively. Please refer to [14] for more detailed expressions for these terms.

To simplify the GN model, we first rewrite (1) as

$$\begin{aligned}\frac{1}{\text{SNR}^{\text{th}}(c_i)} \geq & N_i^{\text{span}} \frac{G_i^{\text{ASE}}}{G_i} + \mu N_i^{\text{span}} G_i^2 \operatorname{arcsinh}\left(\rho \Delta f_i^2\right) \\ & + \mu \sum_{\substack{j \in D \\ j \neq i}} N_{ij}^{\text{span}} G_j^2 \ln \left| \frac{|f_i - f_j| + \Delta f_j/2}{|f_i - f_j| - \Delta f_j/2} \right|, \end{aligned} \tag{2}$$

where μ and ρ are related to fiber parameters [14]. We reasonably assume that (2) is calculated only after the modulation formats, routes, and spectral orderings of all the connections have been determined. Therefore, the left-hand side of (2) is a constant, whereas the right-hand side is a nonlinear function that consists of three different parts describing impairments contributed by the ASE, SCI, and XCI, respectively. Hence, (2) can be expressed as

$$\begin{aligned}\frac{1}{\text{SNR}^{\text{th}}(c_i)} \geq & N_i^{\text{span}} h_1(G_i) + N_i^{\text{span}} h_2(G_i) \\ & + \sum_{\substack{j \in D \\ j \neq i}} N_{ij}^{\text{span}} h_3\left(G_j, \frac{|f_i - f_j|}{\Delta f_j}\right), \end{aligned} \tag{3}$$

for all $i \in D$ with

$$h_1(G_i) = \frac{G_i^{\text{ASE}}}{G_i} \tag{4a}$$

$$h_2(G_i) = \mu G_i^2 \operatorname{arcsinh}\left(\rho \Delta f_i^2\right) \tag{4b}$$

$$h_3\left(G_j, \frac{|f_i - f_j|}{\Delta f_j}\right) = \mu G_j^2 \ln \left| \frac{2|f_i - f_j|/\Delta f_j + 1}{2|f_i - f_j|/\Delta f_j - 1} \right|. \tag{4c}$$

Here, the variables are G_i, G_j, and $|f_i - f_j|/\Delta f_j$ ($|f_i - f_j|/\Delta f_j > 0.5$), whereas $N_i^{\text{span}}, N_{ij}^{\text{span}}$, and Δf_i are constants.

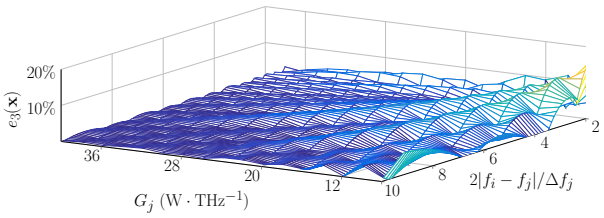

Figure 1. The relative fitting error $e_3(\mathbf{x})$ as a function of G_j and $2|f_i - f_j|/\Delta f_j$. The number of linear functions is set to $Q = 60$.

To linearize the functions in (4), the method described in [26] is used. Specifically, piecewise linear functions [27, Chapter 3] in the form of

$$\hat{h}_u(\mathbf{x}) = \max\{\mathbf{a}_1^T\mathbf{x} + b_1, \ldots, \mathbf{a}_Q^T\mathbf{x} + b_Q\}, \tag{5}$$

are fitted to the nonlinear functions $h_u(\mathbf{x})$ for $u \in \{1, 2, 3\}$. Here Q is the number of linear functions used in the fitting and $\mathbf{x}$ is a vector of variables for $h_u(\mathbf{x})$. $\hat{h}_u(\mathbf{x})$ is much simpler than $h_u(\mathbf{x})$ in numerical computation because it is linear [26]. To guarantee that the resources allocated by the linearized GN model still satisfy the SNR constraints in the original form, the NLIs should be slightly overestimated by $\hat{h}_u(\mathbf{x})$. In other words, $\hat{h}_u(\mathbf{x}) - h_u(\mathbf{x}) \geq 0$ for all $\mathbf{x}$ and $u \in \{1, 2, 3\}$ is required in the linearization.

The quality of the linearization is measured by the relative fitting error defined as $e_u(\mathbf{x}) = (\hat{h}_u(\mathbf{x}) - h_u(\mathbf{x}))/h_u(\mathbf{x})$. The errors are positive such that NLIs are always overestimated and the SNR requirement (1) is satisfied after the linearization. The functions h_1 and h_2 have only one variable and, when $Q = 60$ linear functions are used, their maximum relative fitting errors are 0.4% and 0.1%, respectively. However, h_3 is two-dimensional and, thus, harder to fit. The error $e_3(\mathbf{x})$ is illustrated in Figure 1 with $Q = 60$ and a maximum value of 18.0%. The large fitting error in h_3 does not severely affect the final resource allocation because the intensity of XCI is relatively small compared with other noise terms. The fitting error can be reduced by further increasing the number of linear functions Q in (5) or using more effective linearization algorithms [28].

Table II
PARAMETERS AND VARIABLES IN THE MILP FORMULATION FOR ALL $i, j \in D, l \in E, n \in V$, AND $c \in M$.

Symbol	Meaning
Parameters	
$\varepsilon \in \mathbb{R}^+$	the weight factor that balances the minimizations of the bandwidth usage and total PLI
$v_{i,n} \in \{0, 1\}$	equals 1 if node n is the source or destination of connection i
$z_{l,n} \in \{0, 1\}$	equals 1 if n is an ending node of link l
$\theta \in \mathbb{R}^+$	a large enough number
$R_i \in \mathbb{R}^+$	the bit rate requirement of connection i
$L_l \in \mathbb{N}$	the number of spans in link l
Variables	
$\zeta \in \mathbb{R}^+$	the maximum bandwidth usage
$p_{il} \in \{0, 1\}$	equals 1 if connection i uses link l
$q_{in} \in \{0, 1\}$	equals 1 if connection i goes through node n
$y_{ij} \in \{0, 1\}$	equals 1 if connections i and j share any link
$w_{ijl} \in \{0, 1\}$	equals 1 if connections i and j share link l
$f_i \in \mathbb{R}^+$	the center frequency of connection i
$\Delta f_i \in \mathbb{R}^+$	the bandwidth of connection i
$f_i^{\text{high}} \in \mathbb{R}^+$	the highest frequency used by connection i
$f_i^{\text{low}} \in \mathbb{R}^+$	the lowest frequency used by connection i
$f_{ij} \in \mathbb{R}^+$	the center frequency difference between i and j if $y_{ij} = 1$
$u_{ij} \in \{0, 1\}$	equals 1 if the center frequency of i is higher than j
$m_{ic} \in \{0, 1\}$	equals 1 if i uses modulation format $c \in M$
$\tau_i \in \mathbb{R}^+$	calculates $\operatorname{arcsinh}(\rho \Delta f_i^2)$ for connection i, an auxiliary variable
$t_{ijl}^{\text{XCI}} \in \mathbb{R}^+$	the XCI generated from connection j to i on link l
$t_{il}^{\text{SCI}} \in \mathbb{R}^+$	the SCI of connection i on link l
$t_{il}^{\text{ASE}} \in \mathbb{R}^+$	the ASE of connection i on link l
$t_i^{\text{PLI}} \in \mathbb{R}^+$	the total PLI of connection i
$G_i \in \mathbb{R}^+$	the PSD of connection i

IV. Solution Strategies

Based on the linearized GN model, we first present an MILP formulation in Section IV-A. A heuristic algorithm that decomposes the MILP is then presented in Section IV-B.

A. MILP Formulation

The parameters and variables in the MILP formulation are listed in Table II. The MILP is formulated in (6). Objective (6a) minimizes both the maximum bandwidth usage ζ and the total PLIs of all connections. The balance between these two objectives is controlled by a weight factor ε. A small ε prioritizes the minimization of the bandwidth ζ, while a large ε trades off spectrum resources for robust QoT.

$$\text{minimize} \quad \zeta + \varepsilon \sum_{i \in D} t_i^{\text{PLI}} \tag{6a}$$

subject to

$$\sum_{l \in E} p_{il} z_{l,n} = 2q_{in} - v_{i,n} \qquad \forall i \in D, n \in V \tag{6b}$$

$$\begin{aligned} &p_{il} + p_{jl} \leq 1 + y_{ij} \\ &w_{ijl} \leq p_{il} \\ &w_{ijl} \leq p_{jl} \\ &w_{ijl} \geq p_{il} + p_{jl} - 1 \end{aligned} \qquad \forall l \in E, i, j \in D : i \neq j \tag{6c}$$

$$f_i^{\text{high}} = f_i + \Delta f_i/2 \qquad \forall i \in D \tag{6d}$$

$$f_i^{\text{low}} = f_i - \Delta f_i/2 \qquad \forall i \in D \tag{6e}$$

$$\begin{aligned} &f_i^{\text{low}} + \theta(2 - u_{ij} - y_{ij}) \geq f_j^{\text{high}} \\ &f_{ij} + \theta(2 - u_{ij} - y_{ij}) \geq f_i - f_j \\ &f_{ij} - \theta(2 - u_{ij} - y_{ij}) \leq f_j - f_i \end{aligned} \qquad \forall i, j \in D : i \neq j \tag{6f}$$

$$u_{ij} + u_{ji} = 1 \qquad \forall i, j \in D : i > j \tag{6g}$$

$$\Delta f_i = \sum_{c \in M} \frac{R_i}{c} m_{ic} \qquad \forall i \in D \tag{6h}$$

$$\sum_{c \in M} m_{ic} = 1 \qquad \forall i \in D \tag{6i}$$

$$\tau_i = \sum_{c \in M} m_{ic} \operatorname{arcsinh}(\rho (R_i/c)^2) \qquad \forall i \in D \tag{6j}$$

$$\begin{aligned} &t_{ijl}^{\text{XCI}} + \theta(2 - w_{ijl} - m_{ic}) \\ &\geq \hat{h}_3(G_j, 2m_{ic} c f_{ij}/R_i) L_l \end{aligned} \qquad \begin{aligned} &\forall i, j \in D : i \neq j, \\ &l \in E, c \in M \end{aligned} \tag{6k}$$

$$\begin{aligned} &t_{il}^{\text{SCI}} + \theta(2 - p_{il} - m_{ic}) \\ &\geq \hat{h}_2(G_i) L_l \end{aligned} \qquad \begin{aligned} &\forall i \in D, l \in E, \\ &c \in M \end{aligned} \tag{6l}$$

$$\begin{aligned} &t_{il}^{\text{ASE}} + \theta(2 - p_{il} - m_{ic}) \\ &\geq \hat{h}_1(G_i) L_l \end{aligned} \qquad \begin{aligned} &\forall i \in D, l \in E, \\ &c \in M \end{aligned} \tag{6m}$$

$$\begin{aligned} t_i^{\text{PLI}} \geq{}& \textstyle\sum_{l \in E} (t_{il}^{\text{ASE}} + \mu t_{il}^{\text{SCI}} \tau_i \\ &+ \mu \textstyle\sum_{j \in D, j \neq i} t_{ijl}^{\text{XCI}}) \end{aligned} \qquad \forall i \in D \tag{6n}$$

$$t_i^{\text{PLI}} - \textstyle\sum_{c \in M} m_{ic} / \text{SNR}^{\text{th}}(c) \leq 0 \qquad \forall i \in D \tag{6o}$$

$$f_i^{\text{high}} \leq \zeta \qquad \forall i \in D. \tag{6p}$$

Constraints (6b)–(6g) are related to the routing and spectral ordering assignment. Constraint (6b) is Kirchhoff's law for traffic flows. Constraint (6c) imposes that if two connections i

Table III
PARAMETERS AND VARIABLES IN THE RMLP FOR $i \in D, l \in E$.

Symbol	Meaning
Parameters	
$\Delta f_{ic} \in \mathbb{R}^+$	the bandwidth of connection i using modulation c
P_i	the set of candidate path–modulation pairs for i
P_{il}	the subset of P_i whose paths transverse link l
$(\varsigma, c) \in P_i$	one candidate path–modulation pair for i
$\phi_{i\varsigma c} \in \mathbb{R}$	the NSR margin of path–modulation pair $(\varsigma, c) \in P_i$
$\epsilon_1 \in \mathbb{R}^+$	a positive weight factor in the objective (8a)
$N_{\text{pool}} \in \mathbb{N}$	the size of the RML pool
Variables	
$g_{i\varsigma c} \in \{0, 1\}$	equals 1 if i uses $(\varsigma, c) \in P_i$, otherwise 0
$F_l \in \mathbb{R}^+$	the total bandwidth used by connections using link l
$F_{\text{max}} \in \mathbb{R}^+$	the maximum of F_l among all the links
$\phi_{\text{min}} \in \mathbb{R}^+$	the minimum NSR margin among all the selected path–modulation pairs

and j share link l, then $y_{ij} = 1$ and $w_{ijl} = 1$. Constraints (6d) and (6e) calculate the highest and lowest bandwidths used by each connection. Constraints (6f) and (6g) impose that the spectral ordering of connections should be consistent with their carrier frequencies and bandwidths.

Constraints (6h)–(6p) are related to the physical-layer resource allocation. Constraint (6h) calculates the connection bandwidth. Constraint (6i) guarantees that exactly one modulation format is chosen for one connection. Constraint (6j) creates an auxiliary variable τ_i, which assists the calculation of the SCI. Constraint (6k) implies $t_{ijl}^{\text{XCI}} \geq \hat{h}_3(G_j, 2m_{ic}cf_{ij}/R_i)L_l$ when connection i with modulation format c shares link l with connection j. Constraints (6l) and (6m) imply $t_{il}^{\text{SCI}} \geq \hat{h}_2(G_i)L_l$ and $t_{il}^{\text{ASE}} \geq \hat{h}_1(G_i)L_l$ when connection i uses link l. Constraint (6n) calculates the total PLI. Constraint (6o) ensures that the SNR thresholds are satisfied for all connections, and (6p) calculates an upper bound of spectrum usage among all connections. The inequalities (6k)–(6n) and (6p) are tight in any optimal solution due to the objective function direction as long as $\varepsilon > 0$.

The proposed MILP can be reduced to the routing, modulation level, and spectrum allocation problem, which has been proven NP-complete [6], by replacing Kirchhoff's law for routing with predetermined k-shortest paths and applying transmission reaches instead of the GN model for QoT constraints. Therefore, (6) is also an NP-complete problem and, thus, is unlikely to be solved efficiently [29].

B. Heuristic Algorithm Based on Problem Decomposition

In addition to the MILP formulation, we also propose a low complexity heuristic to solve the resource allocation problem. We decompose (6) into three subproblems: (i) the route and modulation level pooling (RMLP), (ii) the spectral ordering assignment (SOA), and (iii) the frequency and PSD assignment (FPA). The heuristic is summarized by a flowchart in Figure 2.

1) RMLP: The RMLP subproblem takes the traffic requests and network topology as input, and outputs a pool of routing and modulation assignments. All of these candidate assignments are then evaluated in the following SOA and FPA subproblems. The best element in the pool will be chosen as the final solution to the resource allocation problem. As routes and modulations are fixed in the output of RMLP, the values of p_{il}, q_{in}, y_{ij}, w_{ijl}, Δf_i, m_{ic}, and τ_i are determined.

First, the routes and modulations with potentially good QoTs are selected. Given the source and destination nodes of connection i, the k shortest paths can be calculated [30]. Each of the k paths, ς, is combined with all modulation formats $c \in M$, which yields $k|M|$ path–modulation pairs. A subset P_i of these pairs is defined as all (ς, c) whose noise-to-signal ratio (NSR) margin per link

$$\phi_{i\varsigma c} = \frac{1}{N_{i\varsigma}^{\text{span}}} \left(\frac{\phi_0}{\text{SNR}^{\text{th}}(c)} - \text{NSR}_{i\varsigma c}^{\text{est}} \right), \tag{7}$$

is nonnegative. Here $\phi_0, 0 \leq \phi_0 \leq 1$ is a constant representing the maximum tolerable percentage of the ASE and SCI NSRs in the total NSR threshold $1/\text{SNR}^{\text{th}}(c)$. $\text{NSR}_{i\varsigma c}^{\text{est}}$ estimates the lower bound of the actual NSR including the ASE and SCI by

$$\begin{aligned} \text{NSR}_{i\varsigma c}^{\text{est}} &= \min_{G_i} N_{i\varsigma}^{\text{span}} \left(G_i^{\text{ASE}} + \mu G_i^3 \operatorname{arcsinh}\left(\rho \Delta f_{ic}^2\right) \right) / G_i \\ &= 3 N_{i\varsigma}^{\text{span}} \sqrt[3]{\operatorname{arcsinh}\left(\rho \Delta f_{ic}^2\right) / \left(4 (G_i^{\text{ASE}})^2\right)}, \end{aligned}$$

where $\Delta f_{ic} = R_i/c$ is the connection bandwidth, and $N_{i\varsigma}^{\text{span}}$ is the number of spans traversed by path ς. Note that it is hard to calculate the exact XCI before all the resources are allocated. Therefore, we reserve part of the NSR threshold, i.e., $(1 - \phi_0)/\text{SNR}^{\text{th}}(c)$, for the XCI, and select pairs (ς, c) whose $\text{NSR}_{i\varsigma c}^{\text{est}}$ are less than the remaining NSR threshold by (7).

Among the promising candidates in $P_i, i \in D$, the final route and modulation for all the connections are found by the optimization in (8). The parameters and variables in the RMLP optimization are summarized in Table III.

$$\begin{aligned} &\text{minimize} \quad F_{\text{max}} - \epsilon_1 \phi_{\text{min}} && && \text{(8a)} \\ &\text{subject to} \\ &\sum_{(\varsigma,c) \in P_i} g_{i\varsigma c} = 1 && \forall i \in D && \text{(8b)} \\ &F_l = \sum_{i \in D} \sum_{(\varsigma,c) \in P_{il}} \Delta f_{ic} g_{i\varsigma c} && \forall l \in E && \text{(8c)} \\ &F_{\text{max}} \geq F_l && \forall l \in E && \text{(8d)} \\ &\phi_{\text{min}} \leq \sum_{(\varsigma,c) \in P_i} g_{i\varsigma c} \phi_{i\varsigma c} && \forall i \in D. && \text{(8e)} \end{aligned}$$

The weight factor ϵ_1 in (8a) balances the minimization of spectrum usage and maximization of NSR margin. Constraint (8b) enforces that one element in P_i is selected by connection i. Constraint (8c) defines the total bandwidth usage on link l. Constraint (8d) calculates the maximum spectrum among all the links. Constraint (8e) defines the minimum NSR margin. The number of variables and constraints in the RMLP are $O(k|M| \cdot |D|)$ and $O(|D|)$, respectively.

Note that one solution of (8) corresponds to just one route and modulation assignment for all the connections, whereas the candidate pool is formed by solving (8) iteratively N_{pool} times with the previously found solutions excluded during each iteration. Suppose $g_{i\varsigma c}^{\kappa}, \kappa \in \{1, \ldots, K\}$ are the first K solutions obtained by solving (8) K times. The $(K+1)^{\text{th}}$ solution is calculated by solving (8) with the previous K

solutions excluded. Since $\sum_{i\in D,(\varsigma,c)\in P_i} g_{i\varsigma c} = |D|$ (implied by (8b)), adding constraint (8f) to (8) can eliminate solutions with binary variable $g_{i\varsigma c}$ the same as any previous $g^{\kappa}_{i\varsigma c}$

$$\sum_{\substack{i\in D,(\varsigma,c)\in P_i \\ g^{\kappa}_{i\varsigma c}=1}} g_{i\varsigma c} < |D| \qquad \forall \kappa \in \{1,\dots,K\}. \tag{8f}$$

2) SOA: The SOA subproblem takes the traffic requests, network topology, and pool generated from the RMLP as input. For each routing and modulation assignment in the RML pool, the SOA outputs the ordering of connections that share links, i.e., the variable u_{ij} in Table II is determined.

To optimize u_{ij}, disjoint connections, i.e., connections without any shared link, can be partitioned into independent sets (ISs). The indexes of the ISs correspond to their orders on the spectrum. For example, if λ_1 and λ_2 with $\lambda_1 < \lambda_2$ are the indexes of two independent sets, then a connection i in the set IS_{λ_1} will have a lower spectrum order relative to a connection j in the set IS_{λ_2}, or equivalently $u_{ij} = 0$, given that i and j are not disjoint. In addition, observe that connections in the middle of the spectrum usually suffer more XCI from connections on both sides [11]. As a result, pushing connections with low NSR margins $\phi_{i\varsigma c}$ to the outer spectrum ends will reduce the XCI affecting them. This is achieved by a weight factor $w_{i\lambda} = \left[\Lambda^2/4 - (\lambda - \Lambda/2)^2\right]/\phi_{i\varsigma c}$, which gives priority to ISs close the two spectrum extremes if $\phi_{i\varsigma c}$ is small and has a more uniform behavior if $\phi_{i\varsigma c}$ is higher. The SOA described above is solved by an optimization problem in (9).

$$\text{minimize} \quad \bar{f}^{\text{high}} - \bar{f}^{\text{low}} + \epsilon_2 \sum_{i\in D}\sum_{\lambda\in\Lambda} \omega_{i\lambda}\chi_{i\lambda} \tag{9a}$$

subject to

$$\sum_{\lambda\in\Lambda} \chi_{i\lambda} = 1 \qquad \forall i \in D \tag{9b}$$

$$\sum_{i:p_{il}=1} \chi_{i\lambda} \le 1 \qquad \forall l \in E, \lambda \in \Lambda \tag{9c}$$

$$u_{ij} + u_{ji} = 1 \qquad \forall i,j \in D : y_{ij} = 1 \tag{9d}$$

$$u_{ij} \ge \frac{1}{|\Lambda|}\sum_{\lambda\in\Lambda} \lambda\left(\chi_{i\lambda} - \chi_{j\lambda}\right) \qquad \forall i,j \in D : y_{ij} = 1 \tag{9e}$$

$$\bar{f}^{\text{high}}_i - \bar{f}^{\text{low}}_i = \Delta f_i \qquad \forall i \in D \tag{9f}$$

$$\bar{f}^{\text{low}}_i \ge \bar{f}^{\text{high}}_j + \theta\left(u_{ij} - 1\right) \qquad \forall i,j \in D : y_{ij} = 1 \tag{9g}$$

$$\bar{f}^{\text{low}} \le \bar{f}^{\text{low}}_i \qquad \forall i \in D \tag{9h}$$

$$\bar{f}^{\text{high}} \ge \bar{f}^{\text{high}}_i \qquad \forall i \in D \tag{9i}$$

The new parameters and variables in (9) are defined in Table IV. Note that $\bar{f}^{\text{high}}_i$, $\bar{f}^{\text{low}}_i$, $\bar{f}^{\text{high}}$, and $\bar{f}^{\text{low}}$ are only auxiliary variables, the final connection frequencies will be determined in the FPA. Although the exact number of independent sets is not known before the SOA is solved, we can choose Λ large enough, e.g., $\Lambda = |D|$. If fewer sets are used, the empty ones will be removed after the SOA. Objective (9a) minimizes the spectrum usage and XCI simultaneously given $\epsilon_2 > 0$ and $w_{i\lambda} > 0$. Constraint (9b) implies that one connection belongs to exactly one independent set. Constraint (9c) imposes that connections sharing link l are not in the same independent set λ. Constraint (9d) states that either i uses higher independent set index than j or the other way round, if connection i and j share some link (i.e., $y_{ij} = 1$). Constraint (9e) forces u_{ij} to be 1 if the index of the independent set used by i is higher than j. Constraint (9f) calculates the bandwidth of connection i. Constraint (9g) specifies the order of two connections in the spectrum if they share any link. Constraints (9h) and (9i) calculate the spectrum usage of the SOA. The number of variables and constraints in the SOA are both $O(|D|^2)$.

Table IV
PARAMETERS AND VARIABLES IN THE SOA FOR $i, j \in D$.

Symbol	Meaning
Parameters	
$\text{IS}_1, \dots, \text{IS}_\Lambda$	the independent sets with preassigned orders
Λ	the total number of independent sets
$w_{i\lambda}$	$w_{i\lambda} = \left[\Lambda^2/4 - (\lambda - \Lambda/2)^2\right]/\phi_{i\varsigma c}$, a weight factor to reduce the XCI of low NSR margin connections
$y_{ij} \in \{0,1\}$	already defined in Table II as a variable, its value is determined by the routes assigned in the RMLP
$\theta \in \mathbb{R}^+$	a large enough real number
$\epsilon_2 \in \mathbb{R}^+$	a weight factor to balance the minimization of spectrum usage and XCI mitigation in (9)
Variables	
$\chi_{i\lambda} \in \{0,1\}$	equals 1 if i is assigned to independent set λ
$\bar{f}^{\text{high}}$	the maximum frequency used by all the connections
$\bar{f}^{\text{low}}$	the minimum frequency used by all the connections
$\bar{f}^{\text{high}}_i$	the highest frequency used by connection i
$\bar{f}^{\text{low}}_i$	the lowest frequency used by connection i

3) FPA: The frequency and PSD assignment subproblem takes the routing, spectrum, and modulation assignments from the previous subproblem and calculates the optimal frequency and PSD allocation for each element in the RML pool. The one with the minimum spectrum usage among all the candidates is selected as the final solution.

The variables $\zeta, f_i, f^{\text{high}}_i, f^{\text{low}}_i, G_i, t^{\text{XCI}}_{ijl}, t^{\text{SCI}}_{il}, t^{\text{ASE}}_{il}$, and t^{PLI}_i in Table II are determined in the FPA. The variables p_{il}, q_{in}, y_{ij}, w_{ijl}, Δf_i, m_{ic}, τ_i, and u_{ij} are determined in the RMLP and SOA stages and, thus, can be plugged into (6) as constants. The simplified version of (6) is a linear programming problem with continuous variables, which can be easily solved. The number of variables and constraints in the FPA are both $O(|D|^2 \cdot |E|)$.

In summary, the RMLP, SOA, and FPA subproblems are solved sequentially. The output of one subproblem is the input of the next. By combining the routing and modulation assignment from RMLP, the spectral ordering from SOA, and the center frequencies and PSDs in FPA, the final solution is obtained. The pooling strategy tries multiple promising candidate solutions and select the best one among them. By varying the pool size, a trade-off between solving time and solution quality is achieved. Moreover, the complexity of the subproblems can be reduced even further by using approximate heuristic algorithms instead of solving them optimally [7]. Note that the MILP and its decomposed subproblems in (6), (8) and (9) take the connection set D as input and do not assume single flow per node pair. Therefore, connections with the same source and destination nodes are treated separately and different routes, spectra, and PSDs are assigned according to their respective data rate requests.

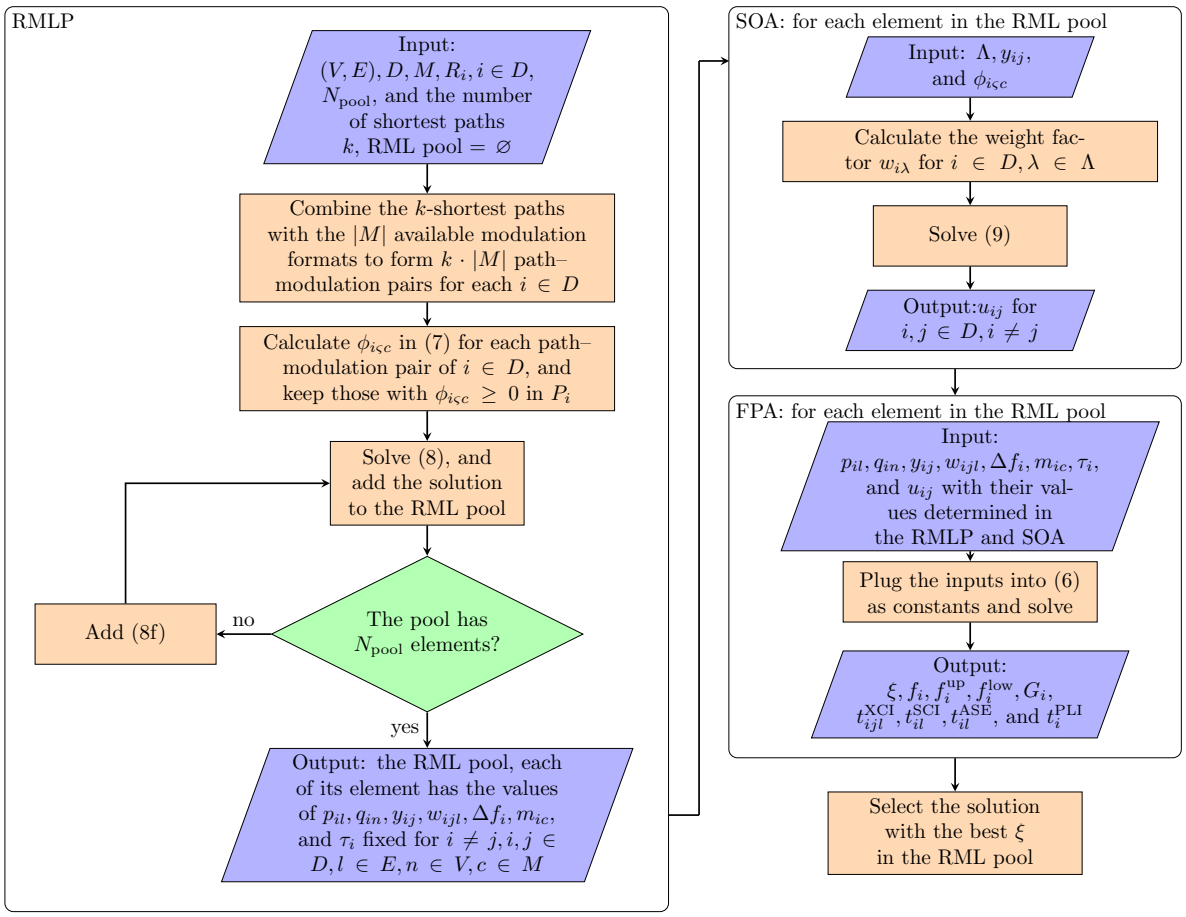

Figure 2. The flowchart of the proposed decomposition heuristic algorithm.

V. Numerical Results

To investigate the performance of our proposed PSD per connection optimization scheme, we consider the uniform PSD allocation as the benchmark. As mentioned before, the benchmark with uniform PSD can be viewed as a special case of our proposed method where an identical PSD value is assigned to every connection. Similar resource allocation schemes with uniform PSD were proposed in [9]–[12].

We consider three topologies for the numerical comparison, a simple 6-node network in Figure 3 and the German and NSF networks [18]. The fiber power attenuation $\alpha = 0.22$ dB$\cdot$km^{-1}, the nonlinear parameter $\gamma = 1.3$ W$^{-1} \cdot$ km^{-1}, the group velocity dispersion $\beta_2 = -21.3$ ps$^2 \cdot$ km^{-1}, the spontaneous emission factor $n_{\text{sp}} = 1.58$ (i.e., the noise figure is 5 dB), the light frequency $\nu = 193.55$ THz and the length of each fiber span L is 100 km. The optimizations are performed by the Gurobi optimizer [31] on a 3.4 GHz quad-core computer with 8 GB RAM memory. The value of ε in (6) is set to 1×10^{-2} for both the MILP and FPA to prioritize the spectrum usage minimization. In the proposed heuristic, we set $\epsilon_1 = 100$ and $\epsilon_2 = 1 \times 10^{-3}$. In the RMLP, the number of shortest paths is $k = 6$ and ϕ_0 is set to 0.9.

The traffic demand of each connection is generated randomly with data rates independently and uniformly distributed from 225 Gbps to 1875 Gbps. For the lowest bit rate request, the connection bandwidth is at least 28.125 GHz (with PM-16QAM), which is higher than the minimum acceptable bandwidth of the GN model (i.e., 28 GHz [23]). The high-bit-rate requests correspond to Nyquist-WDM superchannels formed by multiple subcarriers without guardbands between each other to enable a higher spectral efficiency [20]. The uniform random traffic profile is a widely used assumption [17], [18], [32], [33] to facilitate the numerical evaluation. For each topology, 300 random traffic matrices are used in the simulation. The confidence interval of the simulation results is within 5%, with 95% confidence level.

A. Linearization Errors

First, the quality of the linearization is evaluated by calculating the relative error of the linearized SNRs given by our proposed MILP and heuristic solutions. We assume that there is exactly one connection request per node pair. The relative error is defined as $e_{\text{SNR}} = \left(\text{SNR}^{\text{real}} - \text{SNR}^{\text{linear}}\right)/\text{SNR}^{\text{real}}$ where $\text{SNR}^{\text{linear}} = G_i/t_i^{\text{PLI}}$ is given by solving (6) in the MILP or the FPA stage in the heuristic, and SNR^{real} is the actual SNR

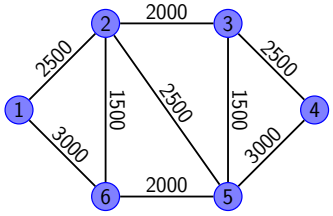

Figure 3. A small network with 6 nodes and 9 links. The number on each link represents the length in kilometers.

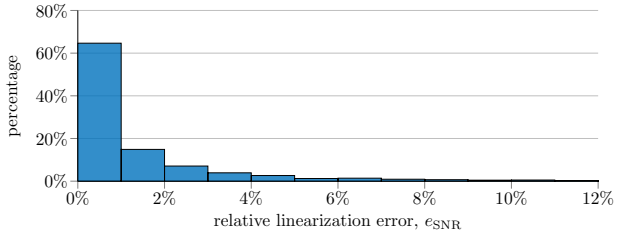

Figure 4. The distribution of relative linearization errors in the proposed MILP solution.

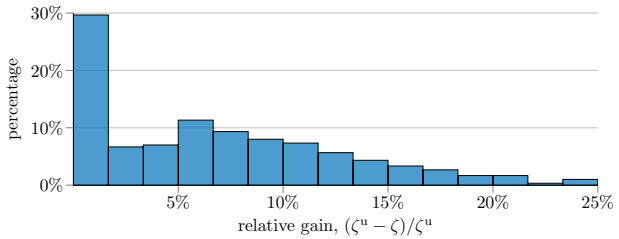

Figure 5. The distribution of relative gain of the proposed MILP compared with the benchmark.

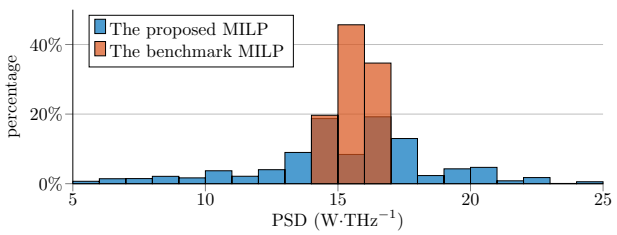

Figure 6. The distribution of PSDs allocated by the proposed MILP and the benchmark MILP.

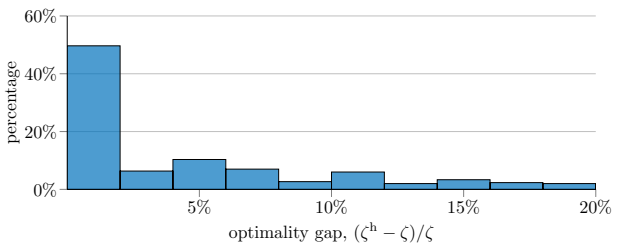

Figure 7. The optimality gap of the proposed heuristic in the small network.

computed using the exact GN model [14].

For the small network in Figure 3, the distribution of e_{SNR} given by the MILP solutions is shown in Figure 4 with an average error of 1.8%. As observed, the error is always positive since the linearization overestimates NLIs. The errors for the NSF and German networks given by the proposed heuristic are also positive with average values of 4.9% and 4.2%, respectively. The larger errors are due to the XCI term, whose linearization error is significantly larger than the other terms in (3) and whose total number increases rapidly as the number of connections in the network grows. The slightly larger error in the NSF compared to the German network can be explained by the larger network diameter of the NSF, because the linearization error also accumulates along the path as indicated by N_i^{span} and N_{ij}^{span} in (3). Nevertheless, the accuracy of the linearized GN model is acceptable and can be used in resource allocations.

B. Small Networks

The optimal resource allocation is investigated by solving the proposed and benchmark MILPs for the small network with one connection request per node pair. The benchmark MILP is performed by solving (6) with the PSDs of all connections constrained to an identical value.

The bandwidth usage of the proposed scheme, ζ, is compared with the bandwidth of the benchmark, ζ^{u}. The relative gain of the proposed MILP, $(\zeta^{\text{u}} - \zeta)/\zeta^{\text{u}}$, is plotted in Figure 5 as a distribution. Here ζ and ζ^{u} are the spectrum usages of the proposed and benchmark MILPs, respectively. The average absolute spectrum usage of the proposed MILP is 380.6 GHz, and its average relative gain is 6.7%. The small average gain of the proposed scheme is due to the simple network topology and small number of connections, which make the NLIs uniform among connections. As the number of connections and the complexity of the network topology increase, the interactions between connections are more severe and the NLIs are diversified. Consequently, the optimal PSDs for different connections will diverge significantly and a scheme with variable PSD per connection will be necessary.

The PSDs allocated by the proposed MILP are spread in a large range as illustrated in Figure 6. One quarter of the connections have PSDs lower than 13.5 W·THz^{-1}, and another quarter of connections have PSDs higher than 17.5 W·THz^{-1}. In contrast, the benchmark allocates uniform PSD within a much narrower range between 14.75 and 16.5 W·THz^{-1} for all the traffic matrices. As illustrated, by diversifying the PSD allocation, the proposed MILP mitigates the NLIs and, thus, improves the resource utilization.

Then we evaluate the proposed heuristic by comparing it with the proposed MILP. In RMLP, we set the pool size $N_{\text{pool}} = 50$. The distribution of the optimality gap $(\zeta^{\text{h}} - \zeta)/\zeta$ between the heuristic and the MILP is shown in Figure 7. The average optimality gap is 4.7%, indicating a good performance of the heuristic algorithm.

C. Large Networks

The performance of the proposed heuristic algorithm is also evaluated in the larger networks with one connection request per node pair. The connection list heuristic [10] with a uniform PSD that minimizes the spectrum usage is chosen as the benchmark scheme. Our proposed heuristic is used with the same parameters as those for the small network except that the pool size is set to $N_{\text{pool}} = 20$ to shorten the runtime. The relative gains of the bandwidth utilization are always positive for all the traffic matrices in both networks. For the NSF network, the average gain and absolute spectrum usage are 19.2% and 4.2 THz, respectively. For the German network, the average gain and absolute spectrum usage are 23.5% and 1.6 THz, respectively. As indicated by the higher relative gains compared with the small network, the individual PSD optimization becomes increasingly important in networks with more nodes and connections, where the NLIs are highly diversified.

The PSDs allocated by the proposed heuristic are compared with the benchmark algorithm in Figure 8 for the German network. A similar distribution is obtained for the NSF network. The proposed heuristic allocates a wide range of PSDs,

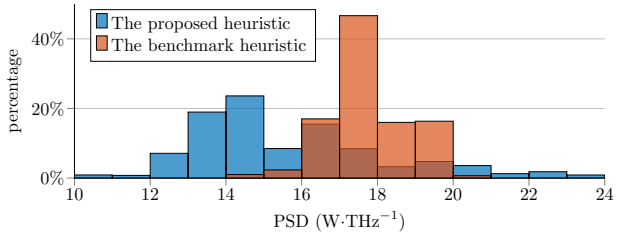

Figure 8. The distributions of allocated PSDs for the proposed and benchmark heuristics in the German network.

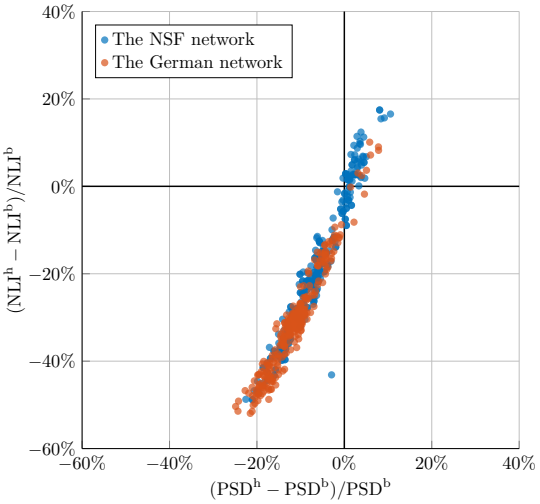

Figure 9. The relative average PSD and NLI differences as a scatter plot for both networks. Each point represents one instance of a simulation with random traffic demands. Here superscript h and b refer to the average values of the proposed and benchmark heuristics, respectively. The average values are based on all the connections in one simulation.

whereas the choice of the benchmark is rather limited. Lower PSDs are used by the proposed heuristic to decrease NLIs in the network.

The relative changes of the NLI and average PSDs between the proposed heuristic and the benchmark are further illustrated in Figure 9, where a scatter plot for both networks is shown. Interestingly, the NLI change in the network is proportional to the PSD change, indicating the importance of PSD optimization to the NLI mitigation. It also shows that lower average PSDs generate lower NLIs and are beneficial in reducing the network resource usage.

Furthermore, we notice that in Figure 9 the points representing the German network are shifted to the bottom left relative to those of the NSF network. This is because the average link length is shorter and, thus, the connections can choose higher-order modulation formats in the German network. As the modulation orders are higher, the SNR thresholds grow exponentially in a linear scale [18] and the margins between the actual SNRs in the benchmark and the thresholds become bigger. Therefore, there is a larger room to reduce connection PSDs for the proposed heuristic to minimize the overall NLI without affecting the spectrum utilization.

Note that the NLI of the proposed heuristic could be worse than that of the benchmark. This is due to the small value of ε in the proposed heuristic, which prioritizes bandwidth minimization over QoT maximization. As a result, the spectrum usage may be decreased in the cost of sacrificed SNR margins. Nevertheless, the QoT requirements are still satisfied since they are hard constraints in the optimizations.

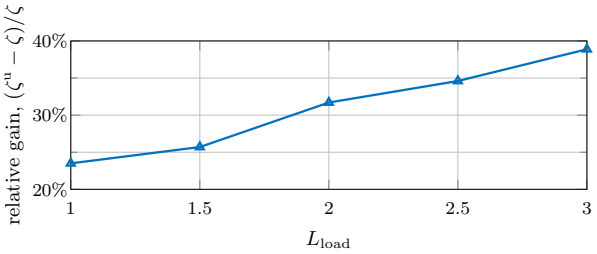

Figure 10. The relative gain of the proposed heuristic compared with the benchmark in the German network as the traffic load L_{load} changes.

D. Multiflow Simulations

To investigate the impact of the traffic load on the algorithm performance, multiflow simulations are performed in the German network, where one node pair may have multiple connection requests. To make the results consistent with the previous single-flow simulations, the traffic demands are generated by first allocating one connection request to each node pair, then add a certain number of connection demands between random node pairs, selected independently with replacement. The traffic load is measured by L_{load}, the ratio between the numbers of total connections and node pairs. The results of the proposed heuristic are compared with the benchmark in Figure 10, where the relative gain grows as L_{load} increases. The running time of the heuristic grows quickly as the load increases, and is in the order of several hours for each instance. The multiflow simulations further illustrate the effectiveness of our proposed methods in heavily loaded networks, where the diversified NLIs generated by a large number of connections can be mitigated by the PSD per connection optimization.

VI. Conclusions

We proposed an MILP formulation and a decomposition heuristic to jointly optimize the routing, spectrum, modulation format, and PSD per connection in flexible-grid optical networks. The nonlinear PLI model is linearized to reduce the computational complexity. The proposed scheme can effectively mitigate NLIs in mesh networks with diverse traffic demands, where impairments are severe and unevenly distributed in the networks. Bandwidth reductions of more than 20% are achieved for the NSF and German networks with the proposed algorithm compared with the uniform PSD benchmark.

References

[1] O. Gerstel, M. Jinno, A. Lord, and S. Yoo, "Elastic optical networking: A new dawn for the optical layer?" *IEEE Communications Magazine*, vol. 50, no. 2, pp. 12–20, 2012.

[2] K. Christodoulopoulos, K. Manousakis, and E. Varvarigos, "Reach adapting algorithms for mixed line rate WDM transport networks," *IEEE Journal of Lightwave Technology*, vol. 29, no. 21, pp. 3350–3363, 2011.

[3] A. Klekamp, R. Dischler, and F. Buchali, "Limits of spectral efficiency and transmission reach of optical-OFDM superchannels for adaptive networks," *IEEE Photonics Technology Letters*, vol. 23, no. 20, pp. 1526–1528, 2011.

[4] X. Wang, M. Brandt-Pearce, and S. Subramaniam, "Impact of wavelength and modulation conversion on transluscent elastic optical networks using MILP," *Journal of Optical Communications and Networking*, vol. 7, no. 7, pp. 644–655, 2015.

[5] E. Palkopoulou, G. Bosco, A. Carena, D. Klonidis, P. Poggiolini, and I. Tomkos, "Nyquist-WDM-based flexible optical networks: Exploring physical layer design parameters," *IEEE Journal of Lightwave Technology*, vol. 31, no. 14, pp. 2332–2339, 2013.

[6] K. Christodoulopoulos, I. Tomkos, and E. Varvarigos, "Elastic bandwidth allocation in flexible OFDM-based optical networks," *IEEE Journal of Lightwave Technology*, vol. 29, no. 9, pp. 1354–1366, 2011.

[7] B. C. Chatterjee, N. Sarma, and E. Oki, "Routing and spectrum allocation in elastic optical networks: a tutorial," *IEEE Communications Surveys & Tutorials*, vol. 17, no. 3, pp. 1776–1800, 2015.

[8] B. C. Chatterjee and E. Oki, "Dispersion-adaptive first–last fit spectrum allocation scheme for elastic optical networks," *IEEE Communications Letters*, vol. 20, no. 4, pp. 696–699, 2016.

[9] H. Beyranvand and J. A. Salehi, "A quality-of-transmission aware dynamic routing and spectrum assignment scheme for future elastic optical networks," *IEEE Journal of Lightwave Technology*, vol. 31, no. 18, pp. 3043–3054, 2013.

[10] J. Zhao, H. Wymeersch, and E. Agrell, "Nonlinear impairment aware resource allocation in elastic optical networks," in *Proc. Optical Fiber Communication Conference (OFC)*, Los Angeles, CA, 2015, pp. M2I–1.

[11] L. Yan, E. Agrell, H. Wymeersch, P. Johannisson, R. Di Taranto, and M. Brandt-Pearce, "Link-level resource allocation for flexible-grid nonlinear fiber-optic communication systems," *IEEE Photonics Technology Letters*, vol. 27, no. 12, pp. 1250–1253, June 2015.

[12] J. Zhao, H. Wymeersch, and E. Agrell, "Nonlinear impairment-aware static resource allocation in elastic optical networks," *IEEE Journal of Lightwave Technology*, vol. 33, no. 22, pp. 4554–4564, 2015.

[13] L. Yan, E. Agrell, and H. Wymeersch, "Resource allocation in nonlinear flexible-grid fiber-optic networks," in *Proc. Optical Fiber Communication Conference (OFC)*, Los Angeles, CA, 2015, pp. Tu2I–5.

[14] L. Yan, E. Agrell, H. Wymeersch, and M. Brandt-Pearce, "Resource allocation for flexible-grid optical networks with nonlinear channel model," *Journal of Optical Communications and Networking*, vol. 7, no. 11, pp. B101–B108, 2015.

[15] I. Roberts, J. Kahn, and D. Boertjes, "Convex channel power optimization in nonlinear WDM systems using Gaussian noise model," *IEEE Journal of Lightwave Technolog*, vol. 34, no. 13, pp. 3212–3222, 2016.

[16] D. J. Ives, P. Bayvel, and S. J. Savory, "Adapting transmitter power and modulation format to improve optical network performance utilizing the Gaussian noise model of nonlinear impairments," *IEEE Journal of Lightwave Technology*, vol. 32, no. 21, pp. 3485–3494, 2014.

[17] D. J. Ives, P. Bayvel, and S. J. Savory, "Physical layer transmitter and routing optimization to maximize the traffic throughput of a nonlinear optical mesh network," in *Proc. IEEE International Conference of Optical Network Design and Modeling (ONDM)*, Stockholm, Sweden, May 2014, pp. 168–173.

[18] D. J. Ives, P. Bayvel, and S. J. Savory, "Routing, modulation, spectrum and launch power assignment to maximize the traffic throughput of a nonlinear optical mesh network," *Photonic Network Communications*, vol. 29, no. 3, pp. 244–256, 2015.

[19] *Spectral grids for WDM applications: DWDM frequency grid*, Telecommunication Standardization Sector of International Telecommunication Union Recommendation ITU-T G.694.1, 2012.

[20] D. Hillerkuss, R. Schmogrow, M. Meyer, S. Wolf, M. Jordan, P. Kleinow, N. Lindenmann, P. C. Schindler, A. Melikyan, X. Yang *et al.*, "Single-laser 32.5 Tbit/s Nyquist WDM transmission," *Journal of Optical Communications and Networking*, vol. 4, no. 10, pp. 715–723, 2012.

[21] P. Poggiolini, "The GN model of non-linear propagation in uncompensated coherent optical systems," *IEEE Journal of Lightwave Technology*, vol. 30, no. 24, pp. 3857–3879, 2012.

[22] P. Poggiolini, G. Bosco, A. Carena, V. Curri, Y. Jiang, and F. Forghieri, "The GN-model of fiber non-linear propagation and its applications," *IEEE Journal of Lightwave Technology*, vol. 32, no. 4, pp. 694–721, 2014.

[23] P. Johannisson and E. Agrell, "Modeling of nonlinear signal distortion in fiber-optic networks," *IEEE Journal of Lightwave Technology*, vol. 32, no. 23, pp. 3942–3950, 2014.

[24] R. Schmogrow, M. Winter, M. Meyer, D. Hillerkuss, S. Wolf, B. Baeuerle, A. Ludwig, B. Nebendahl, S. Ben-Ezra, J. Meyer *et al.*, "Real-time Nyquist pulse generation beyond 100 Gbit/s and its relation to OFDM," *Optics Express*, vol. 20, no. 1, pp. 317–337, 2012.

[25] P. Johannisson and M. Karlsson, "Perturbation analysis of nonlinear propagation in a strongly dispersive optical communication system," *IEEE Journal of Lightwave Technology*, vol. 31, no. 8, pp. 1273–1282, 2013.

[26] A. Magnani and S. P. Boyd, "Convex piecewise-linear fitting," *Optimization and Engineering*, vol. 10, no. 1, pp. 1–17, 2009.

[27] S. Boyd and L. Vandenberghe, *Convex optimization*. Cambridge University Press, 2004.

[28] E. Amaldi, S. Coniglio, and L. Taccari, "Discrete optimization methods to fit piecewise affine models to data points," *Computers and Operations Research*, vol. 75, pp. 214–230, 2016.

[29] D. S. Johnson, "A brief history of NP-completeness, 1954–2012," *Documenta Mathematica*, pp. 359–376, 2012.

[30] J. Y. Yen, "Finding the k shortest loopless paths in a network," *Management Science*, vol. 17, no. 11, pp. 712–716, 1971.

[31] Gurobi Optimization, Inc., "Gurobi optimizer reference manual," http://www.gurobi.com, 2015.

[32] A. Alvarado, D. J. Ives, S. J. Savory, and P. Bayvel, "On optimal modulation and FEC overhead for future optical networks," in *Proc. Optical Fiber Communication Conference (OFC)*, Los Angeles, CA, 2015, pp. Th3E–1.

[33] S. Talebi, E. Bampis, G. Lucarelli, I. Katib, and G. N. Rouskas, "Spectrum assignment in optical networks: A multiprocessor scheduling perspective," *Journal of Optical Communications and Networking*, vol. 6, no. 8, pp. 754–763, 2014.